Acousto-optic couplings in two-dimensional phoxonic crystal cavities

Quentin Rolland, M. Oudich, Said El-Jallal, Samuel Dupont, Yan Pennec, Joseph Gazalet, Jean-Claude Kastelik, Gaëtan Lévêque, Bahram Djafari-Rouhani

Acousto-optic couplings in two-dimensional phoxonic crystal cavities

Cite as: Appl. Phys. Lett. **101**, 061109 (2012); https://doi.org/10.1063/1.4744539
Submitted: 25 June 2012 • Accepted: 26 July 2012 • Published Online: 09 August 2012

Q. Rolland, M. Oudich, S. El-Jallal, et al.

Acousto-optic couplings in two-dimensional phoxonic crystal cavities

Q. Rolland,[1] M. Oudich,[2] S. El-Jallal,[2] S. Dupont,[1] Y. Pennec,[2] J. Gazalet,[1] J. C. Kastelik,[1] G. Lévêque,[2] and B. Djafari-Rouhani[2]
[1]*Institut d'Electronique, de Microélectronique et de Nanotechnologie, UMR CNRS 8520, Université de Valenciennes-Hainault-Cambresis, Valenciennes, France*
[2]*Institut d'Electronique, de Microélectronique et de Nanotechnologie, UMR CNRS 8520, UFR de Physique, Université Lille 1, Villeneuve d'Ascq, France*

(Received 25 June 2012; accepted 26 July 2012; published online 9 August 2012)

We investigate the acousto-optic coupling, based on both photo-elastic and opto-mechanical mechanisms, in periodic structures with simultaneous photonic and phononic band gaps. The investigations are focused on a cavity defect in which the strong confinement of acoustic and optic waves enhances the interaction. We calculate the modulation of each photonic mode frequency by each phononic mode confined in the cavity. We compare the strength for the photo-elastic and opto-mechanical effects in the different cases. Both mechanisms can be in phase or out of phase and produce additive or subtractive effects in the total acousto-optic coupling. © *2012 American Institute of Physics*. [http://dx.doi.org/10.1063/1.4744539]

Artificial periodic structures enable the design of materials that exhibit band gaps for photons or phonons, the so called photonic[1,2] and phononic[3–5] crystals. One may also consider the design of a photonic crystal for the near infrared telecommunication bands that behaves as a phononic crystal for acoustic waves in the hypersonic range of 1–10 GHz. In particular, the existence of simultaneous elastic and electromagnetic band gaps in the latter frequency ranges have been studied in the last few years. Maldovan and Thomas[6,7] have shown theoretically that dual photonic and phononic band gaps can easily be obtained in two-dimensional (2D) square and hexagonal lattice crystals made of silicon matrix drilled with air holes. In general, the photonic band gaps are not absolute but are obtained for either transverse electric TE (out-of-plane electric field) and transverse magnetic TM (in-plane electric field) polarizations of the light. The existence of absolute band gaps has been examined by Bria *et al.*,[8] using the anisotropy of the dielectric matrix in sapphire in the microwave regime. Sadat-Saleh *et al.*[9] have studied the gaps dependence on size of the pattern added in the unit cell and its impact on the existence of simultaneous band gaps.

Dual phononic-photonic (also called phoXonic) crystals as well as opto-mechanical structures are of great interest as they allow integrated devices with enhanced acousto-optic interaction. Opto-mechanical effects in crystal slabs that sustain both optical and mechanical excitations have been widely studied during the last few years.[10–13] Periodic slabs containing linear and cavity defects[14–16] in which the confinement of both excitations or the existence of slow modes can allow the enhancement of phonon-photon interaction have also been reported. Finally, some papers are dealing with the possibility of enhanced phonon-photon interaction in one-dimensional strip waveguides.[10,17,18]

The above structures pave the way towards efficient and fast control of photons by phonons in compact phoXonic structures. It is expected that the high level of energy confinement in these structures enhances photo-elastic and opto-mechanic coupling phenomena. Indeed, an acoustic wave induces a variation of the refractive index due to the elastic strain (the well-known Pockels effect[19]) and elastic energy confinement will lead to a strengthened index variation. In addition, when the electromagnetic energy is trapped in a high quality cavity, the mechanical displacement of the cavity boundaries modulates the resonant frequency of the optical cavity.[20]

In this letter, we investigate the modulation of an optical wave through the photo-elastic and opto-mechanic effects in a phoXonic cavity. More precisely, we study the dependence of the optical cavity eigenmodes on the spatial distribution and symmetry of the acoustical modes. We show that the strength of the acousto-optic interaction depends on the choice of the acoustic and optic modes of the cavity. Moreover, the photo-elastic and opto-mechanical effects can contribute differently and, in particular, act in phase or out of phase. The results presented in this paper are computed using the finite element method (FEM) for a 2D square lattice crystal consisting of infinite air holes in a silicon matrix. We first describe the phoXonic structure and the acousto-optic interaction implementation. Then, the most significant results are presented and discussed followed by some general conclusions.

A prerequisite for the search of cavity modes is the existence of band gaps in both photonic and phononic defect free crystals (without cavity). Indeed wide band gaps promote the likelihood of simultaneous confinement of acoustical and optical modes. Previous studies[6,21] of 2D crystals consisting of holes in a silicon matrix indicate that a ratio of the radius r of the cylinders to the lattice period a around 0.48 seems to be a good candidate. This ratio corresponds to a filling factor f (defined as $f = \pi r^2/a^2$) of 0.72. It shows simultaneous complete and sufficiently large band gaps for acoustic modes composed of mixed shear and longitudinal vibrations in the x-y plane (in-plane vibrations) as well as for TE and TM optical polarizations.

We create a cavity in the perfect crystal by removing one hole. Then, the acoustic and optical eigenfrequencies and eigenvectors of the cavity are calculated using the super-cell method.[7,20] A 7×7 super-cell provides a good

compromise between the accuracy of the results and a reasonable computation time. It appears that TM optical modes display better energy confinement than TE modes. So, in this paper, we will concentrate on the phonon-photon interaction involving the TM optical cavity modes.

When a localized acoustic mode of the cavity is excited, the frequencies of the optical TM modes undergo a modulation around their values for the unperturbed cavity. Two coexisting mechanisms, involving the local variation of the dielectric permittivity, are responsible of this acousto-optic effect: the photo-elastic and the opto-mechanical effects. The former is due to the acoustic strain via the Pockels effect,[18,22] whereas the latter takes into account the dynamic motion of the silicon-vacuum boundaries around the holes.[13,20]

We use a quasi-static approximation to characterize the acousto-optic interaction. This is justified by the fact that the optical frequency ω is by several order of magnitude higher than the acoustical frequency Ω. So, we re-calculate the optical cavity modes at several selected instants of an acoustical period, the acoustic mode profile being frozen at these instants.

Concerning Pockels effect, we determine the variation of the relative permittivity $\Delta\varepsilon_{ij}$ corresponding to each frozen strain distribution. Considering the m3m symmetry of silicon and the in-plane (i.e., x-y plane) acoustic modes in our 2D structure, the $\Delta\varepsilon_{ij}$ are given by,[18]

$$\begin{aligned}\Delta\varepsilon_{11} &= -\varepsilon^2(S_1p_{11} + S_2p_{12})\\ \Delta\varepsilon_{22} &= -\varepsilon^2(S_1p_{12} + S_2p_{11})\\ \Delta\varepsilon_{33} &= -\varepsilon^2(S_1p_{12} + S_2p_{12})\\ \Delta\varepsilon_{12} &= \Delta\varepsilon_{21} = -\varepsilon^2S_6p_{44}\\ \Delta\varepsilon_{13} &= \Delta\varepsilon_{23} = \Delta\varepsilon_{31} = \Delta\varepsilon_{32} = 0,\end{aligned} \tag{1}$$

where the $p_{\alpha\beta}$ are the material photo-elastic constants and S_β the acoustic strain according to Voigt notations. As concerns the opto-mechanical effect, we simply recalculate the eigenmodes for successive frozen deformations of the structure geometry during one acoustic period. For silicon, we have used the following values of the photo-elastic parameters: $p_{11} = -0.1$, $p_{12} = 0.01$, and $p_{44} = -0.051$.[23] The other used material parameters are: the mass density $\rho = 2331\,\mathrm{kg/m^3}$, the three independent stiffness coefficients $c_{11} = 16.57 \times 10^{10}$, $c_{12} = 6.39 \times 10^{10}$, and $c_{44} = 7.962 \times 10^{10}\,\mathrm{N/m^2}$, the optical refractive index $n = 3.46$ and the transverse velocity of sound $v_t = 5840\,\mathrm{m/s}$ (Ref. 23) in silicon.

Figures 1 and 2 illustrate the eigenfrequencies of the cavity modes in the band diagrams together with the corresponding mode profiles respectively for the acoustic field and the TM polarized optic field. Due to the band folding inherent to the supercell approach, the band structure appears somewhat dense in the propagative region. For clarity, these figures are mainly restricted around the band gaps region whose edges have been delimited by black dashed lines. Also, they are drawn only along one of the high symmetry directions (ΓX) of the irreducible Brillouin zone since the branches associated with localized modes are flat and independent of the wave vector. We label these cavity modes in ascending order using capital letters for the phononic modes and lowercase Greek letters for the TM optical modes.

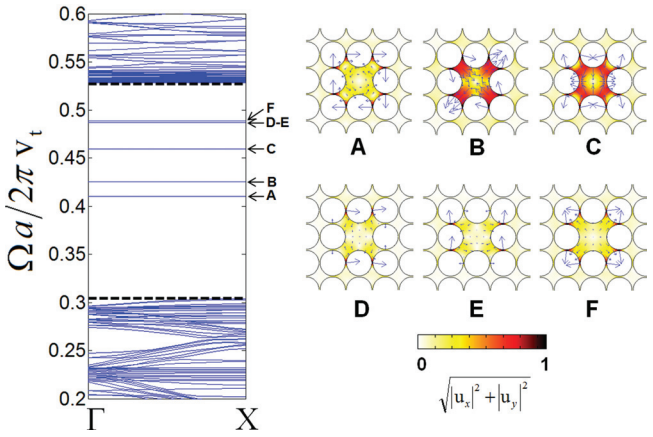

FIG. 1. Eigenfrequencies of the six acoustic cavity modes in the band structure and the maps of their displacement fields in the x-y plane. For each cavity mode, the blue arrows indicate the displacement field vector $\vec{u} = (u_x, u_y)$ for specific spatial positions in the silicon cavity.

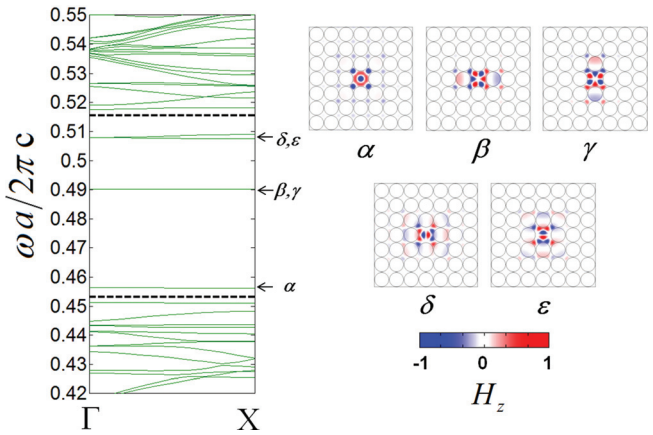

FIG. 2. Eigenfrequencies of the TM optical cavity modes and the maps of their magnetic field H_z.

As shown in Figure 1, six phononic eigenfrequencies are located in the forbidden band-gap and the corresponding mode profiles display a good confinement inside the cavity. As expected, the main deformation introduced by each of the confined acoustic mode is essentially localized inside and in the vicinity of the cavity. For instance, mode A appears essentially as a shear strained mode where the cavity is twisted back and forth during an acoustic period ($0 < \Omega t < 2\pi$ where t is the time). Concerning the mode B, its time evolution results in a deformation of the cavity in such a way that one of its diagonals is stretched and the other contracted during one half of the acoustic period. Then, in the next half-period the stretched diagonal becomes contracted and vice versa. During each half acoustic period, the mode labeled C initially of almost square shape is alternatively expanded along one of its side lengths and contracted in the other. We also notice a marked distortion at the four cavity corners. The modes, D and E, are degenerate and their distribution profiles are orthogonal. Finally, the time evolution of the mode labeled F shows to be essentially a breathing mode without too much distortion of the cavity shape.

Considering the TM modes, three of them are relatively well confined as shown in Figure 2. The first one α is a single mode followed by two degenerated modes β and γ. The next

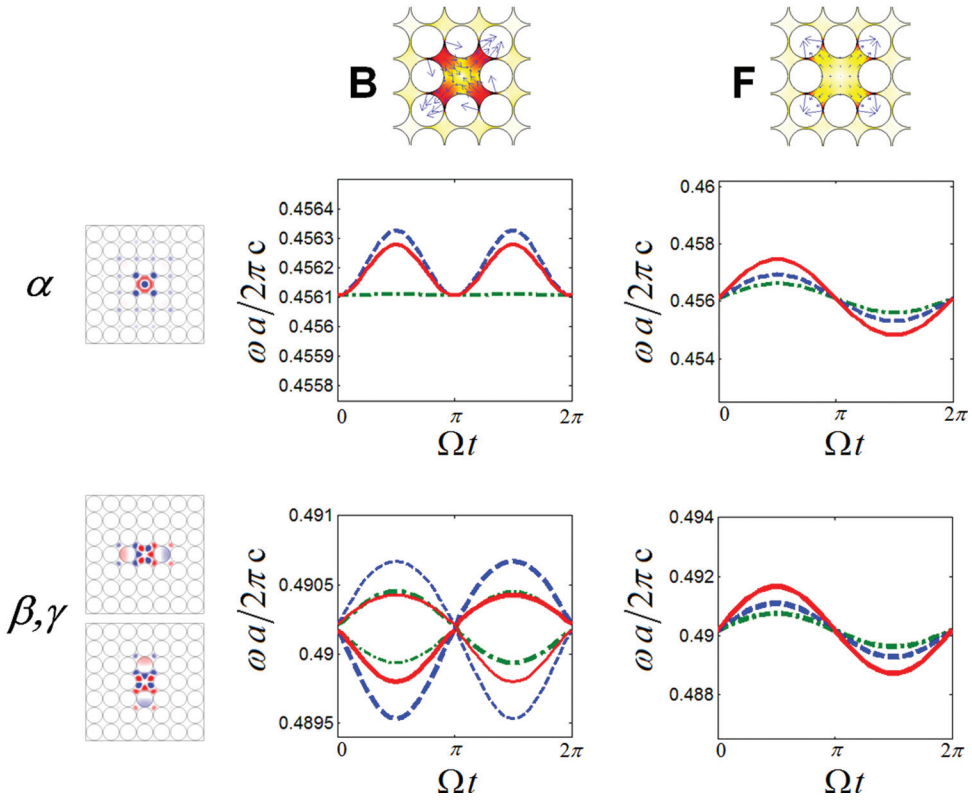

FIG. 3. Modulations of the TM modes α, β, and γ frequencies by the acoustic modes B and F. The figures present the oscillations of the α (upper panels) and β, γ (lower panels) modes as a function of Ωt during one period of the acoustic mode. The left and right panels give respectively the results for the B and F acoustic modes. The red-solid curves represent the end results when both interaction mechanisms are taken into consideration while blue-dashed and green-dashed-dotted lines stand respectively for opto-mechanic and photo-elastic effects acting alone. In the lower panels, thin and thick lines differentiate the two degenerate modes β and γ.

modes δ and ε are also degenerate but less localized than the former modes. This results in a small lift of their degeneracy in the band structure plot due to a weak interaction between cavities in the neighboring cells.

We have calculated the acousto-optic interaction between the above localized phonons and photons. In this work, we analyze the interaction of the acoustic modes B and F with the non degenerate optical mode α and the doubly degenerate modes β and γ. Indeed, these cases provide the strongest interaction and cover at the same time the main variety of situations that can be met. For each acoustic mode, we fix the maximum of the deformation in the cavity at 1% and calculate the modulation of the TM optical modes during one acoustic period ($0 < \Omega t < 2\pi$). The results are presented in Figure 3. In order to compare the strength of both acousto-optic mechanisms, we present on the same figure their individual contributions calculated independently (green and blue curves for photo-elastic and opto-mechanical effects, respectively) together with the overall results when both effects are taken into account at the same time (red curves). Also, thick and thin lines have been used to distinguish between the time evolution of the eigenfrequencies of the two degenerate modes β and γ.

We notice that the acoustic modes B and F have qualitatively different effects on the optic modes. The breathing acoustic mode F produces an almost sinusoidal modulation of each of the optical modes α, β and γ, while the degeneracy of the latter modes is conserved. In contrast, the modulation of the optic mode α by the acoustic mode B resembles the square of a sinusoidal function (or equivalently a sinusoid with frequency of 2Ω instead of Ω). The evolution of modes β and γ displays the shape of a slightly distorted sinusoidal function and their degeneracy is lifted.

Symmetry considerations associated to the perturbation theory provide a simple interpretation of these results.[20] To give a better insight into the time evolution of the acoustic modes B and F, we show in Figure 4 the maps of their displacement fields at the time $\Omega t = \pi/2$. Since the mode F conserves the symmetry of the cavity, it will not lift the degeneracy of the optical modes. The breathing character of this mode will change the volume of the cavity and, in turn, the frequencies of the optical modes will increase or decrease during the contraction and dilatation of the cavity, respectively. As concerns the acoustic mode B, the symmetry of its displacement field with respect to the symmetry axes of the cavity is such that the first order acousto-optic perturbation vanishes for the optic mode α, thus resulting in a second order effect that manifests itself in the square sinusoidal function of the modulation curve in Fig. 3(a). On the other hand, there is a first order correction on the frequencies of modes β and γ but in this case, the second order effect is not negligible and produces a flattening of the sinusoidal curve

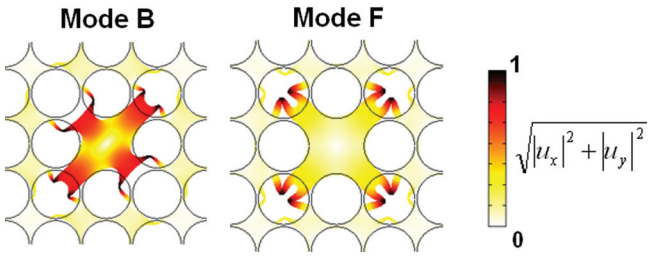

FIG. 4. Spatial distribution of the total in-plane acoustic displacement in the cavity for modes B and F, respectively, at $\Omega t = \pi/2$ in a 7×7 supercell. To illustrate the opto-mechanical effect, the structure deformation has been oversized in the entire domain. The background represents the unperturbed structure.

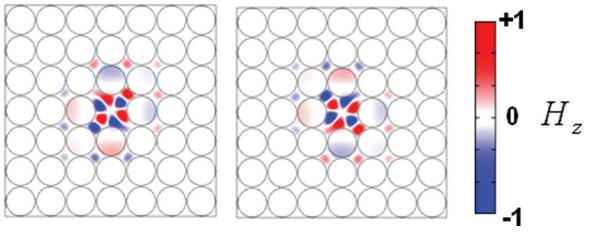

FIG. 5. Maps of the magnetic fields for the hybrid modes β' and γ' in presence of the perturbation introduced by the acoustic mode B at $\Omega t = \pi/2$.

as the superposition of a sine and a squared sine function of Ωt. Also, the symmetry of the original cavity is broken causing the lifting of the degeneracy of the optical frequencies. In the presence of the acoustic mode B, the new eigenmodes are hybrid optical modes, i.e., linear combination of the unperturbed modes β and γ. The profiles of these resulting hybrid modes which we label β' and γ', are given in Figure 5. In the present case, these linear combinations are found to be very close to a simple superposition: $\beta \pm \gamma$.

Concerning the strength of the two acousto-optic mechanisms, one can notice that the opto-mechanical effect is predominant in all the cases considered here, although both effects are of the same order of magnitude. Obviously, when the two effects are taken into account the computed results for the combined effects are somewhat different from a simple addition or subtraction of their individual contributions. When the cavity is perturbed by the acoustic mode F, the two effects are in phase and strengthen the acousto-optic interaction as can be seen in Figure 3 for the phononic/photonic pairs (F, $\beta - \gamma$) and (F, α). In contrast, the two effects are out of phase for the pairs (B, $\beta - \gamma$). Finally in the case of the pair (B, α), the photo-elastic effect alone is negligible even at the second order.

In conclusion, we present the study of the acousto-optic effects in silicon phoXonic crystals. We evaluate the impact of the perturbation introduced by an acoustic mode confined in a cavity on the optical modes localized in this same cavity. The choice of the two interacting modes turns to have a strong impact on the modulation of the optical mode frequencies, i.e., their response to the acoustic perturbation. An interpretation of the different encountered situations is given based on symmetry considerations and the theory of perturbations. Also, for the chosen examples, we observe that the opto-mechanic effect is the predominant interaction mechanism and, depending on the interacting modes profiles, opto-mechanic and photo-elastic mechanisms can either sustain each other or on the contrary display counteracted effects.

This work has been carried out within the phoXcry project n°ANR-09-NANO-004 funded by the French National Agency (ANR) in the frame of its 2009 programme in Nanosciences, Nanotechnologies and Nanosystems (P3N2009). The authors from University of Lille (MO, SEJ, YP, GL, and BDR) acknowledge the support of the European Commission Seventh Framework Programs (FP7) under the FET-Open project TAILPHOX N 233883.

[1]E. Yablonovitch, Phys. Rev. Lett. **58**, 2059 (1987).
[2]J. D. Joannopoulos, S. G. Johnson, J. N. Winn, and R. D. Meade, *Photonic Crystals: Molding the Flow of Light* (Princeton University Press, 2008).
[3]M. S. Kushwaha, P. Halevi, L. Dobrzynski, and B. Djafari-Rouhani, Phys. Rev. Lett. **71**, 2022 (1993).
[4]M. M. Sigalas and E. N. Economou, Solid State Commun. **86**, 141 (1993).
[5]Y. Pennec, J. Vasseur, B. Djafari-Rouhani, L. Dobrzynski, and P. A. Deymier, Surf. Sci. Rep. **65**, 229 (2010).
[6]M. Maldovan and E. L. Thomas, Appl. Phys. B **83**, 595 (2006).
[7]M. Maldovan and E. L. Thomas, Appl. Phys. Lett. **88**, 251907 (2006).
[8]D. Bria, M. B. Assouar, M. Oudich, Y. Pennec, J. Vasseur, and B. Djafari-Rouhani, J. Appl. Phys. **109**, 014507 (2011).
[9]S. Sadat-Saleh, S. Benchabane, F. I. Baida, M. P. Bernal, and V. Laude, J. Appl. Phys. **106**, 074912 (2009).
[10]M. Eichenfield, J. Chan, R. M. Camacho, K. J. Vahala, and O. Painter, Nature **462**, 78 (2009).
[11]A. H. Safavi-Naeini and O. Painter, Opt. Express **18**, 14926 (2010).
[12]E. Gavartin, R. Braive, I. Sagnes, O. Arcizet, A. Beveratos, and T. J. Kippenberg, Phys. Rev. Lett. **106**, 203902 (2011).
[13]D. A. Fuhrmann, S. M. Thon, H. Kim, D. Bouwmeester, P. M. Petroff, A. Wixforth, and H. J. Krenner, Nature Photon. **5**, 605 (2011).
[14]S. Mohammadi, A. A. Eftekhar, A. Khelif, and A. Adibi, Opt. Express **18**, 9164 (2010).
[15]Y. Pennec, B. Djafari-Rouhani, E. H. El Boudouti, C. Li, Y. El Hassouani, J. O. Vasseur, N. Papanikolaou, S. Benchabane, V. Laude, and A. Martinez, Opt. Express **18**, 14301 (2010).
[16]V. Laude, J.C. Beugnot, S. Benchabane, Y. Pennec, B. Djafari-Rouhani, N. Papanikolaou, J. M. Escalante, and A. Martinez, Opt. Express **19**, 9690 (2011).
[17]Y. Pennec, B. Djafari-Rouhani, C. Li, J. M. Escalante, A. Martinez, S. Benchabane, V. Laude, and N. Papanikolaou, AIP Adv. **1**, 041901 (2011).
[18]P. T. Rakich, C. Reinke, R. Camacho, P. Davids, and Z. Wang, Phys. Rev. X **2**, 011008 (2012).
[19]D. Royer and E. Dieulesaint, *Elastic Waves in Solids II: Generation, Acousto-optic Interaction, Applications* (Springer, 1999).
[20]S. G. Johnson, M. Ibanescu, M. A. Skorobogatiy, O. Weisberg, J. D. Joannopoulos, and Y. Fink. Phys. Rev. E **65**, 066611 (2002).
[21]Q. Rolland, S. Dupont, J. Gazalet, D. Yudistira, J.-C. Kastelik, and Y. Pennec, "Modelisation of Acousto-optic Interaction in 2D Phoxonic Crystal," in Oecd Conference Center, Paris, France, 8–10 February 2012, OPTRO-2012-095.
[22]A. Yariv and P. Yeh, *Optical Waves in Crystals* (Wiley, New York, 1984).
[23]D. K, Biegelsen, Phys. Rev. B **32**, 1196 (1974).